

# PROCEEDINGS OF SPIE

[SPIDigitalLibrary.org/conference-proceedings-of-spie](https://SPIDigitalLibrary.org/conference-proceedings-of-spie)

## Symbol-by-symbol maximum likelihood (ML) detection with reduced complexity over multicarrier systems

Tsai, Shang-Ho, Yu, Xiaoli, Kuo, C.-C.

Shang-Ho Tsai, Xiaoli Yu, C.-C. Jay Kuo, "Symbol-by-symbol maximum likelihood (ML) detection with reduced complexity over multicarrier systems," Proc. SPIE 5440, Digital Wireless Communications VI, (10 August 2004); doi: 10.1117/12.541979

**SPIE.**

Event: Defense and Security, 2004, Orlando, Florida, United States

# Symbol-by-Symbol Maximum Likelihood (ML) Detection with Reduced Complexity over Multicarrier Systems

Shang-Ho Tsai, Xiaoli Yu and C.-C. Jay Kuo

Department of Electrical Engineering and Signal and Image Processing Institute  
University of Southern California, Los Angeles, CA 90089-2564, USA

## ABSTRACT

A symbol-by-symbol maximum likelihood (ML) detection scheme for multicarrier (MC) systems is proposed in this work. When the number of subchannels is sufficiently large, the received symbols across all subchannels are approximately uncorrelated. Then, the proposed symbol-by-symbol ML detection, which is obtained by minimizing the symbol error probability, is nearly optimal. Furthermore, we will show how to reduce the complexity of the symbol-by-symbol ML detection when the constellation size is large. Simulation results show that the proposed symbol-by-symbol ML detection scheme outperforms the symbol-by-symbol minimum distance (MD) detection scheme by up to 2 dB in a noisy environment with crosstalk such as the DMT-ADSL system.

## 1. INTRODUCTION

Multicarrier (MC) systems are widely adopted in both wireline and wireless communications recently,<sup>1,2,3</sup> The MC systems divide a channel into subchannels using DFT (discrete Fourier transform) and IDFT (inverse discrete Fourier transform) matrices. When the number of subchannels is sufficiently large, the received symbols across all subchannels are approximately uncorrelated even the underlying noise is not additive white Gaussian noise (AWGN).<sup>4</sup> Consequently, detection can be conducted symbol by symbol with good accuracy.

Nowadays, the symbol-by-symbol detection scheme used in many MC systems is based on the minimum distance (MD) criterion, *i.e.* choosing the constellation point that is closest to the received symbol as the transmitted symbol. However, the performance of the symbol-by-symbol MD detection scheme may deteriorate since the real and imaginary parts of each received symbol are in general correlated.<sup>5</sup> This is due to the fact that the real and imaginary parts of the received noise are correlated.

A symbol-by-symbol maximum likelihood (ML) detection scheme for the MC systems is proposed in this work. When the number of subchannels is sufficiently large, such a detection scheme, which is formulated by minimizing the symbol error probability, is nearly optimal. Since the symbol-by-symbol ML detection scheme uses exhaustive search for all possible constellations and then choose the most possible one, the complexity grows quickly when a high bit rate is used. In this work, we shown that it is adequate to consider only the four most closest constellation points of the received symbol so that exhaustive search can be avoided. We will demonstrate this claim using the DMT-ADSL system. Simulation results show that the symbol-by-symbol ML detection scheme can outperform the symbol-by-symbol MD detection scheme by up to 2 dB in an noise environment with crosstalk.

## 2. SYSTEM MODEL

In this section, we will review the DMT (Discrete Multi-Tone) system briefly and then analyze the correlation between the real and imaginary parts of a received symbol is in general not zero. Before moving on, let us first introduce some notations to be used throughout this paper.

1. **Boldfaced** lowercases and **Boldfaced** uppercases denote vectors or matrices, respectively.
2.  $\mathbf{A}^t$  denotes the transpose of  $\mathbf{A}$ .
3.  $\text{Trace}\{A\}$  and  $\text{Det}\{A\}$  denote the trace and the determinant of  $\mathbf{A}$ , respectively.
4.  $E\{x\}$  denotes the expectation of the random variable  $x$ .
5.  $\text{Re}\{x\}$  and  $\text{Im}\{x\}$  denote the real part and the imaginary part of  $x$ , respectively.

6.  $\text{var}\{x\}$  denotes the variance of random variable  $x$ .

The block-diagram of a DMT system is shown in Fig. 1, where CP, P/S and TEQ denote the cyclic prefix, the parallel-to-serial conversion and the time-domain equalization. The one-tap multiplication after the IDFT matrix is usually called the frequency-domain equalization (FEQ).

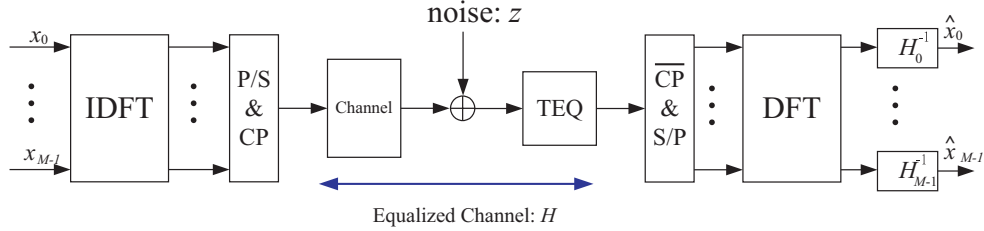


**Figure 1.** The block-diagram of a DMT system.

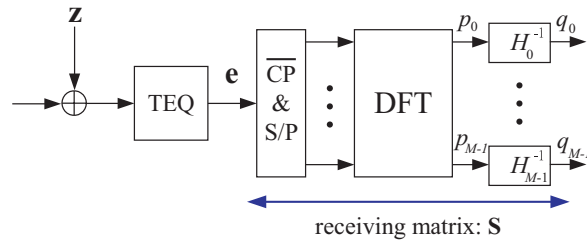


**Figure 2.** The block-diagram of the received noise path.

Let us consider the receive noise path as shown in Fig. 2, where  $M$  is the number of subchannels and  $L$  the length of CP. The path from the TEQ output to the FEQ output can be represented by a receive matrix:<sup>7</sup>

$$\mathbf{S} = \mathbf{\Gamma}^{-1} \left( \begin{array}{c|c} \mathbf{0} & \mathbf{W} \\ \hline M \times L & M \times M \end{array} \right), \quad (1)$$

where  $\mathbf{\Gamma}$  is the  $M \times M$  diagonal matrix whose diagonal elements are the frequency response of the equalized channel and  $\mathbf{W}$  is the  $M \times M$  unitary discrete Fourier transform (DFT) matrix whose element in the  $k$ th row and the  $n$ th column is given by

$$[\mathbf{W}]_{kn} = \frac{1}{\sqrt{M}} e^{-j \frac{2\pi}{M} kn} \quad \text{for } 0 \leq k, n \leq M-1. \quad (2)$$

Let  $\mathbf{s}_k^t$  be the  $k$ th row of  $\mathbf{S}$ , i.e.  $\mathbf{S} = [\mathbf{s}_0 \ \mathbf{s}_1 \ \dots \ \mathbf{s}_{M-1}]^t$ . The noise at the  $k$ th subchannel of the FEQ output can be expressed as

$$\begin{aligned} q_k &= \mathbf{s}_k^t \mathbf{e} \\ &= \underbrace{\text{Re}\{\mathbf{s}_k^t \mathbf{e}\}}_{\text{Re}\{q_k\}} + j \underbrace{\text{Im}\{\mathbf{s}_k^t \mathbf{e}\}}_{\text{Im}\{q_k\}}, \end{aligned} \quad (3)$$

where  $\mathbf{e}$  is the noise vector at the TEQ output.

The correlation coefficient of  $\text{Re}\{q_k\}$  and  $\text{Im}\{q_k\}$  is defined by

$$\rho_k = \frac{E\{\text{Re}\{q_k\} \text{Im}\{q_k\}\}}{\sqrt{\text{var}\{\text{Re}\{q_k\}\} \text{var}\{\text{Im}\{q_k\}\}}}. \quad (4)$$

The numerator of  $\rho_k$  is the cross correlation between  $Re\{q_k\}$  and  $Im\{q_k\}$ , which can be computed via

$$\begin{aligned} E\{Re\{q_k\}Im\{q_k\}\} &= E\{Re\{\mathbf{s}_k^t \mathbf{e}\}Im\{\mathbf{s}_k^t \mathbf{e}\}\} \\ &= E\{Re\{\mathbf{s}_k^t\} \mathbf{e} \mathbf{e}^t Im\{\mathbf{s}_k\}\} \\ &= Re\{\mathbf{s}_k^t\} \mathbf{R}_{ee} Im\{\mathbf{s}_k\}, \end{aligned} \quad (5)$$

where  $\mathbf{R}_{ee}$  is the correlation matrix of  $\mathbf{e}$ . Next, let us examine the denominator of  $\rho_k$  in Eqn. (4). Using a derivation similar to that for Eqn. (5), we have

$$var\{Re\{q_k\}\} = Re\{\mathbf{s}_k^t\} \mathbf{R}_{ee} Re\{\mathbf{s}_k\}, \quad (6)$$

and

$$var\{Im\{q_k\}\} = Im\{\mathbf{s}_k^t\} \mathbf{R}_{ee} Im\{\mathbf{s}_k\}. \quad (7)$$

Based on (4), (5), (6), and (7), the noise correlation at the  $k$ th subchannel is given by

$$\rho_k = \frac{Re\{\mathbf{s}_k^t\} \mathbf{R}_{ee} Im\{\mathbf{s}_k\}}{\sqrt{Re\{\mathbf{s}_k^t\} \mathbf{R}_{ee} Re\{\mathbf{s}_k\}} \sqrt{Im\{\mathbf{s}_k^t\} \mathbf{R}_{ee} Im\{\mathbf{s}_k\}}}. \quad (8)$$

Let  $\mathbf{z}$  be the noise vector before TEQ with the correlation matrix  $\mathbf{R}_{zz}$  and  $N_t$  be the TEQ length. Let us examine the relationship between  $\mathbf{R}_{zz}$  and  $\mathbf{R}_{ee}$  using the matrix representation. By using the property of the linear convolution, the elements from 0 to  $M - 1$  of  $\mathbf{e}$  are affected by the elements from  $-N_t + 1$  to  $M - 1$  of  $\mathbf{z}$ . More specifically, we have

$$\underbrace{\begin{pmatrix} e(0) \\ e(1) \\ \vdots \\ e(M-1) \end{pmatrix}}_{\mathbf{e}} = \underbrace{\begin{pmatrix} t_{N_t-1} & \dots & t_0 & 0 & \dots & 0 \\ 0 & & t_1 & t_0 & & \\ \vdots & & \ddots & & \ddots & \vdots \\ 0 & \dots & & t_{N_t-1} & \dots & t_0 \end{pmatrix}}_{\mathbf{T}} \underbrace{\begin{pmatrix} z(-N_t+1) \\ \vdots \\ z(-1) \\ z(0) \\ \vdots \\ z(M-1) \end{pmatrix}}_{\mathbf{z}}, \quad (9)$$

where  $\mathbf{T}$  is of dimension  $M \times (M + N_t - 1)$  and  $\mathbf{z}$  is of dimension  $(M + N_t - 1) \times 1$ . From (9), we can derive the relationship between  $\mathbf{R}_{zz}$  and  $\mathbf{R}_{ee}$  as

$$\mathbf{R}_{ee} = \mathbf{T} \mathbf{R}_{zz} \mathbf{T}^t. \quad (10)$$

As given by (8),  $Re\{q_k\}$  and  $Im\{q_k\}$  are uncorrelated only when  $Re\{\mathbf{s}_k^t\} \mathbf{R}_{ee} Im\{\mathbf{s}_k\} = 0$ . In an MC system, even if  $\mathbf{z}$  is uncorrelated,  $Re\{q_k\}$  and  $Im\{q_k\}$  is in general correlated since the real and imaginary parts of FEQ are usually unequal, which leads to unequal attenuation for  $Re\{q_k\}$  and  $Im\{q_k\}$ . Moreover,  $\mathbf{z}$  is often correlated, e.g. the crosstalk effect in DMT systems. Thus, the correlation between  $Re\{q_k\}$  and  $Im\{q_k\}$  becomes even more complicated.

In Sec. 4, we will show in Example 1 that the absolute value of  $\rho_k$  can approach to unity in some subchannels of a crosstalk environment. In other words, the real and imaginary parts of the received noise are highly correlated. We will also show that the noise variances of the real and imaginary parts are usually not the same. In this situation, symbol-by-symbol MD detection is not optimal and will have performance degradation. To improve the detection performance, we will propose a symbol-by-symbol ML detection. When the number of subchannels is sufficiently large, the noise vector at the FEQ output can be assumed to be uncorrelated so that symbol-by-symbol ML detection will not have much performance degradation as compared with block-by-block ML detection.

### 3. SYMBOL-BY-SYMBOL ML DETECTION WITH REDUCED COMPLEXITY

In this section, we propose the symbol-by-symbol ML detection scheme. The complexity of such a scheme grows as an exponential function of the constellation size, if an exhaustive search is used to find the most possible symbol

for each received input symbol. However, we show that it is possible to consider only the four closest constellation points of the received symbol at the cost of little performance loss.

Let the  $2 \times 1$  vectors  $(Re\{x_k\} Im\{x_k\})^t$  and  $(Re\{\hat{x}_k\} Im\{\hat{x}_k\})^t$  be represented by  $\mathbf{x}_k$  and  $\hat{\mathbf{x}}_k$ , respectively. Given that each element in the noise vector  $\mathbf{z}$  is a Gaussian random variable, the received symbols at the FEQ output are also Gaussian random variables, whose probability density function at the  $k$ th subchannel is given by

$$Pr(\hat{\mathbf{x}}_k|\mathbf{x}_k) = \frac{1}{2\pi\sqrt{\det\{\mathbf{C}_k\}}} \exp\left\{-\frac{1}{2}(\hat{\mathbf{x}}_k - \mathbf{x}_k)^t \mathbf{C}_k^{-1}(\hat{\mathbf{x}}_k - \mathbf{x}_k)\right\}, \quad (11)$$

where  $\mathbf{C}_k$  is the  $2 \times 2$  noise covariance matrix at the  $k$ th subchannel given by

$$\mathbf{C}_k = \begin{pmatrix} \sigma_{Re\{q_k\}}^2 & \rho_k \sigma_{Re\{q_k\}} \sigma_{Im\{q_k\}} \\ \rho_k \sigma_{Re\{q_k\}} \sigma_{Im\{q_k\}} & \sigma_{Im\{q_k\}}^2 \end{pmatrix}, \quad (12)$$

and where  $\sigma_{Re\{q_k\}}^2$  and  $\sigma_{Im\{q_k\}}^2$  are the real and imaginary parts of the noise variance, respectively. Using the eigen-decomposition, we obtain

$$\mathbf{C}_k = \mathbf{E}_k \mathbf{\Lambda}_k \mathbf{E}_k^t, \quad (13)$$

where  $\mathbf{E}_k$  is the eigen-matrix with its columns consisting of eigenvectors  $\mathbf{e}_k(1)$  and  $\mathbf{e}_k(2)$ , and  $\mathbf{\Lambda}_k$  is a diagonal matrix with its diagonal elements equal to eigenvalues  $\lambda_k(1)$  and  $\lambda_k(2)$ . Let  $b_k$  be the bit allocated to the  $k$ th subchannel. Hence, there are  $2^{b_k}$  possible constellation points denoted by  $\mathbf{x}_k[0], \dots, \mathbf{x}_k[2^{b_k} - 1]$  at the  $k$ th subchannel. Therefore, the ML decision rule which selects the most possible constellation point  $\mathbf{x}_k^{ML}$  is given by

$$\mathbf{x}_k^{ML} = \arg \left\{ \min_m \left\{ (\hat{\mathbf{x}}_k - \mathbf{x}_k[m])^t \mathbf{C}_k^{-1} (\hat{\mathbf{x}}_k - \mathbf{x}_k[m]) \right\} \right\}, \quad 0 \leq m \leq 2^{b_k} - 1. \quad (14)$$

Eliminating common terms in (14), the ML decision rule becomes

$$\mathbf{x}_k^{ML} = \arg \left\{ \min_m \left\{ \hat{\mathbf{x}}_k^t \mathbf{C}_k^{-1} \mathbf{x}_k[m] - \frac{1}{2} \|\mathbf{x}_k[m]\|^2 \right\} \right\}, \quad 0 \leq m \leq 2^{b_k} - 1. \quad (15)$$

To determine the most possible transmitted symbol with exhaustive search, we should compute the function with  $2^{b_k}$  constellations as given in Eqn. (15) and then choose the constellation point that minimizes the function. Thus, the complexity of the symbol-by-symbol ML detection is of  $\mathcal{O}(2^{b_k})$  per symbol. That is, subchannels with higher bit rates will suffer from higher complexity than that of lower rates. In DMT-ADSL systems, the bit allocation per symbol can be as high as 15 bits. It seems impractical to adopt exhaustive search in implementing the symbol-by-symbol ML detection scheme in this situation.

Fortunately, the complexity can be greatly reduced under constraints. We will use the DMT-ADSL system to illustrate this point. In DMT systems, the symbol error probability at each subchannel should be the same to achieve the optimal performance and the symbol error probability is demanded to be smaller than a certain value, which is denoted by  $\alpha$ . Now, let us derive the maximum distance between the transmitted and received symbols at the  $k$ th subchannel if the symbol error probability is constrained to be less than  $\alpha$ . The derived maximum distance can be used to determine how many closest constellation points of the received symbol should be considered instead of exhaustive search.

From (11) and (12), we have

$$\begin{aligned} & \frac{1}{2\pi\sqrt{\det\mathbf{C}_k}} \exp\left\{-\frac{1}{2}(\hat{\mathbf{x}}_k - \mathbf{x}_k)^t \mathbf{C}_k^{-1}(\hat{\mathbf{x}}_k - \mathbf{x}_k)\right\} < \alpha \\ \Rightarrow & (\hat{\mathbf{x}}_k - \mathbf{x}_k)^t \mathbf{C}_k^{-1}(\hat{\mathbf{x}}_k - \mathbf{x}_k) > 2 \ln \left( \frac{1}{2\pi\alpha \sigma_{Re\{q_k\}} \sigma_{Im\{q_k\}} \sqrt{1 - \rho_k^2}} \right) \\ \Rightarrow & \frac{(v_k(1) - \hat{v}_k(1))^2}{\lambda_k(1)} + \frac{(v_k(2) - \hat{v}_k(2))^2}{\lambda_k(2)} > 2 \ln \left( \frac{1}{2\pi\alpha \sigma_{Re\{q_k\}} \sigma_{Im\{q_k\}} \sqrt{1 - \rho_k^2}} \right), \end{aligned} \quad (16)$$

where  $(v_k(1) v_k(2))^t = \mathbf{E}_k \mathbf{x}_k$  and  $(\hat{v}_k(1) \hat{v}_k(2))^t = \mathbf{E}_k \hat{\mathbf{x}}_k$ . For a given transmitted symbol, the probability distribution function of the received symbol can be represented by contours as shown in Fig 3. The center of the contours is the

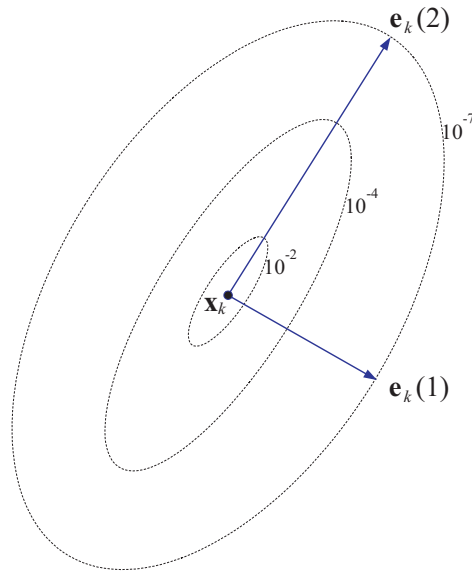


**Figure 3.** The contours of the conditional probability  $Pr(\hat{\mathbf{x}}_k|\mathbf{x}_k)$ .

transmitted symbol  $\mathbf{x}_k$  and the probability on the same contour is the same. Given the position of the transmitted symbol, the contours can help to determine the probability of the received symbol  $\hat{\mathbf{x}}_k$ .

Without loss of generality, let us assume  $\lambda_k(2) > \lambda_k(1)$  in the following discussion. In any fixed contour, the maximum distance between  $\mathbf{x}_k$  and  $\hat{\mathbf{x}}_k$  occurs when the vector  $\mathbf{x}_k - \hat{\mathbf{x}}_k$  lies along the direction of  $\mathbf{e}_k(2)$  as depicted in Fig. 4. Let the maximum distance be  $d_{k,max}$ . From (16),  $d_{k,max}$  can be obtained by setting

$$(v_k(1) - \hat{v}_k(1)) = 0 \text{ and } d_{k,max} = |v_k(2) - \hat{v}_k(2)|.$$

Thus, with a fixed symbol error probability  $\alpha$ , the square of the maximum distant is given by

$$\begin{aligned} d_{k,max}^2 &= (v_k(2) - \hat{v}_k(2))^2 \\ &= 2\lambda_k(2) \ln \left( \frac{1}{2\pi\alpha \sigma_{Re\{q_k\}} \sigma_{Im\{q_k\}} \sqrt{1 - \rho_k^2}} \right). \end{aligned} \quad (17)$$

As given in Eqn. (17),  $d_{k,max}^2$  can be interpreted as the maximum possible noise variance at the  $k$ th subchannel for a constrained error probability  $\alpha$  and a given noise covariance matrix  $\mathbf{C}_k$ .

Next, let us examine the signal-to-noise ratio (SNR) at the FEQ output of the  $k$ th subchannel. It is defined by

$$SNR_k = \frac{\mathcal{E}_k}{\sigma_{Re\{q_k\}}^2 + \sigma_{Im\{q_k\}}^2}, \quad (18)$$

where  $\mathcal{E}_k$  is the average transmit energy at the  $k$ th subchannel. Assume QAM is used and let the minimum distance between  $\mathbf{x}_k$  be  $\Delta_k$ , where  $0 \leq k \leq M - 1$ . The transmitted energy at the  $k$ th subchannel can be expressed by<sup>4</sup>

$$\mathcal{E}_k = \frac{(2^{b_k} - 1)\Delta_k^2}{6}. \quad (19)$$

From (18) and (19), we obtain

$$\Delta_k = \left[ SNR_k \frac{6 \text{Trace}\{\mathbf{C}_k\}}{(2^{b_k} - 1)} \right]^{1/2}. \quad (20)$$

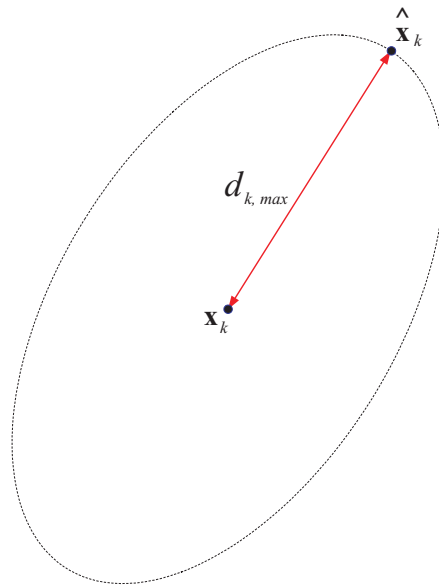


**Figure 4.** The maximum distance between  $\hat{\mathbf{x}}_k$  and  $\mathbf{x}_k$ .

Note that  $\Delta_k$  is also the minimum distance between  $\hat{\mathbf{x}}_k$  if the system is ISI (inter-symbol-interference) free. Therefore, based on (17) and (20), we can compare the two values and use their relative strength to determine the number of possible constellation points to examine (instead of exhaustive search).

One example to show the relative positions of the maximum possible distance of the received symbol and the minimum distance of the transmitted symbol is given in Fig. 5. In Sec. 4, we will show in Example 2 that it is adequate to consider only four closest constellation points of the received symbol in a typical DMT-ADSL system.

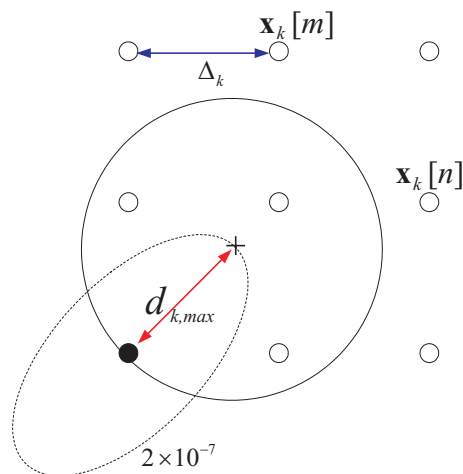


**Figure 5.** The relationship between  $d_{k,max}$  and  $\Delta_k$ .

## 4. SIMULATION RESULTS

### 4.1. Example 1: Performance Comparison between ML and MD Detectors

The example demonstrates the performance improvement using symbol-by-symbol ML detection in the DMT-ADSL system. Let the sampling frequency be 2.208 MHz and  $M = 512$  and the constellation be 4-QAM. The channel impulse response and the corresponding frequency response of CSA Loop #6 are shown in Fig. 6. The TEQ length is equal to 20, and the non-iterative TEQ algorithm that maximizes the signal to interference ratio (*SIR*) of the equalized channel impulse response<sup>8</sup> is adopted. The equalized channel impulse response and the corresponding frequency response are shown in Fig. 7. The power spectrum density (PSD) of HDSL near-end crosstalk with 10 disturbers is shown in Fig. 8.

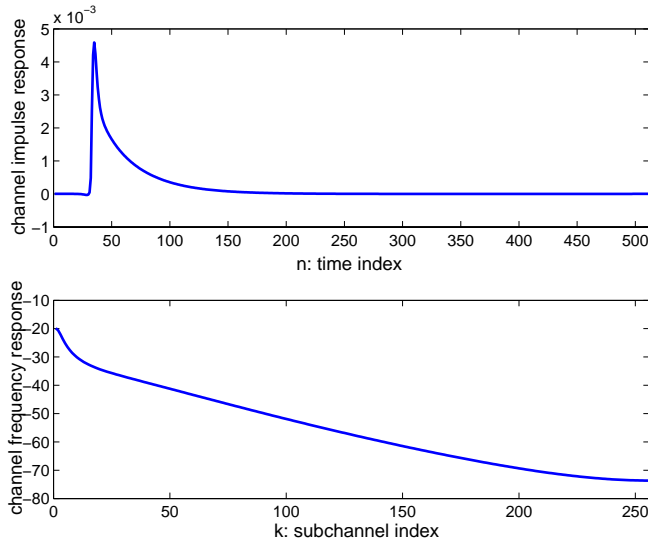


**Figure 6.** The channel impulse response and the corresponding frequency response of CSA Loop #6.

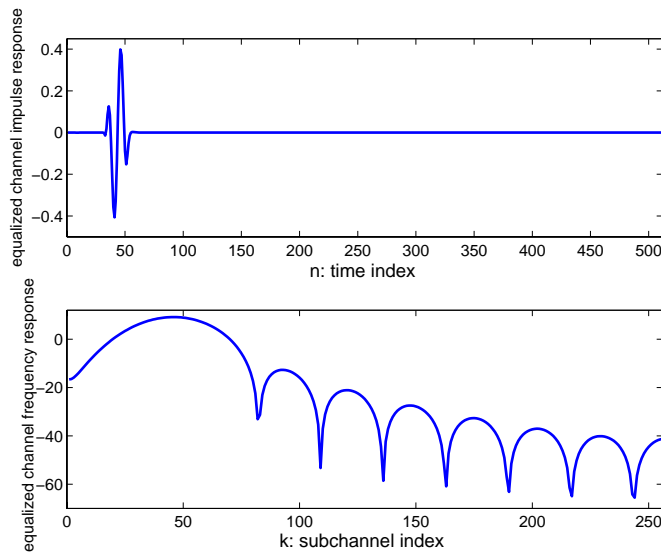


**Figure 7.** The equalized channel impulse response and the corresponding frequency response of CSA Loop #6.



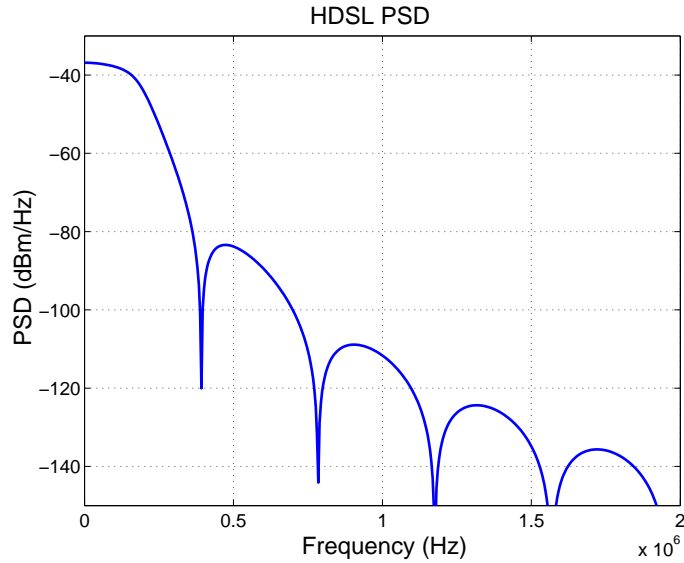


**Figure 8.** The power spectral density (PSD) of HDSL near-end crosstalk with 10 disturbers.

Under the conditions stated above, the correlation coefficient  $\rho_k$  can be calculated according to Eqn. (8). It is plotted as a function of subchannel index  $k$  in Fig. 9. The normalized noise variance of the real and imaginary parts at each subchannel is shown in Fig. 10.

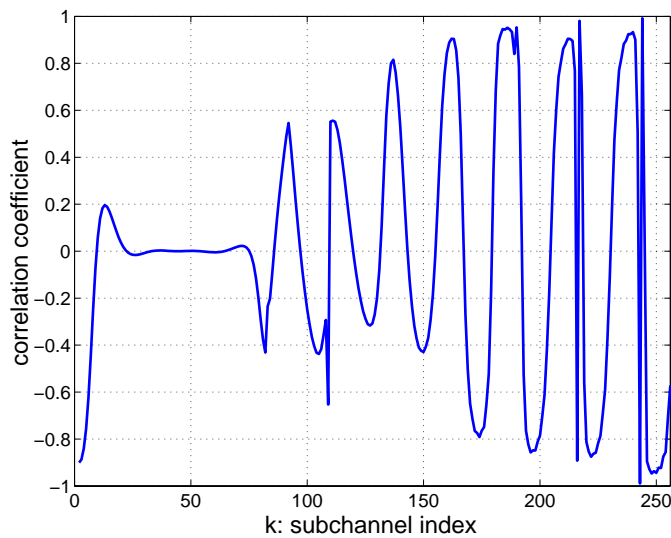


**Figure 9.** The correlation coefficient as a function of the subchannel index.

From Figs. 9 and 10, the correlation coefficient at subchannel  $k = 112$  is  $\rho_{112} = 0.5$  and the variance difference between the real and the imaginary parts of  $q_{112}$  is  $|\text{var}\{\text{Re}\{q_{112}\}\} - \text{var}\{\text{Im}\{q_{112}\}\}| = 1 \text{ dB}$ . The performance comparison between the symbol-by-symbol ML and MD detectors for subchannel  $k = 112$  using numerical simulation is shown in Fig. 12. We see that the symbol-by-symbol ML detection improves the performance by about 1 dB. Let us examine another subchannel with  $k = 211$ . From Figs. 9 and 10, we see  $\rho_{211} = 0.9$  and  $|\text{var}\{\text{Re}\{q_{211}\}\} - \text{var}\{\text{Im}\{q_{211}\}\}| = 3 \text{ dB}$ . The performance comparison using numerical simulation for subchannel  $k = 211$  is given in Fig. 11, where the performance improvement is more than 2 dB.

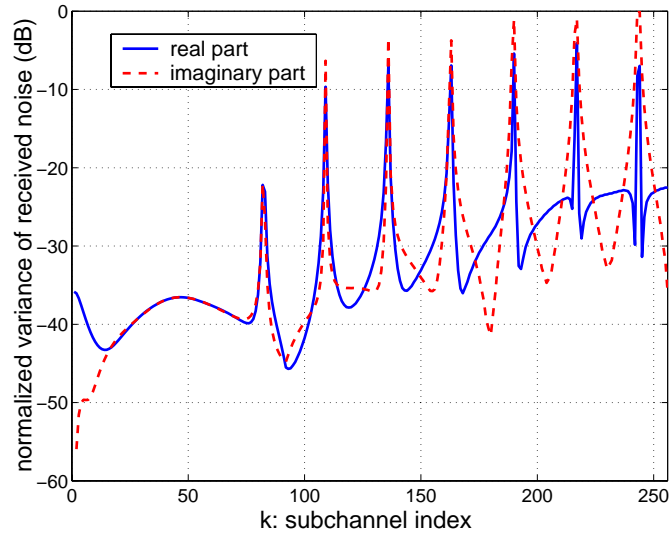


**Figure 10.** The normalized variance of the real and imaginary parts of each subchannel.

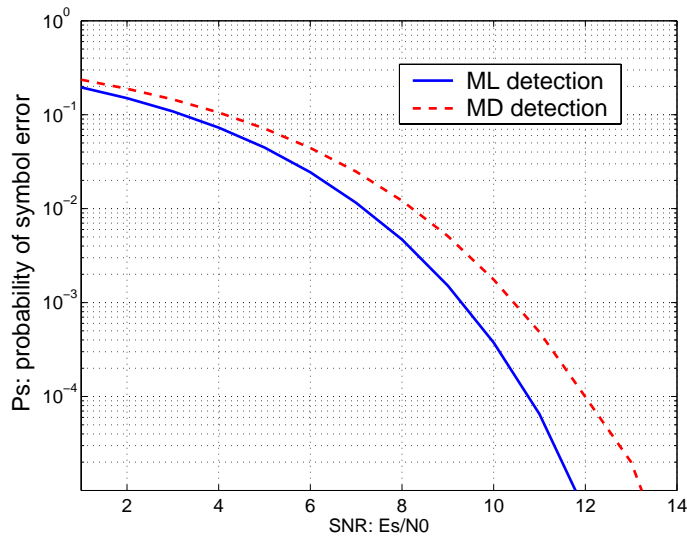


**Figure 11.** The performance evaluation of the symbol-by-symbol ML and MD detector with 4-QAM at subchannel  $k = 112$ .

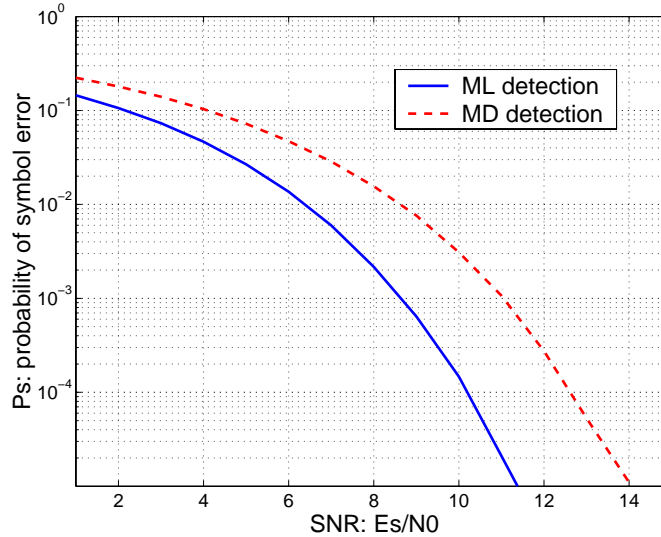


**Figure 12.** The performance evaluation of the symbol-by-symbol ML and MD detectors with 4-QAM at subchannel  $k = 211$ .

#### 4.2. Example 2: Complexity Reduction of Symbol-by-Symbol ML Detection

In this example, we would like to show that it is adequate to consider only the four closest constellation points of the received symbol instead of using exhaustive search under the symbol error rate constraint demanded by DMT-ADSL. In DMT-ADSL, the transmitted symbols are QAM symbols. The minimum bit allocation is 2 bits which requires  $SNR$  greater than 14.5 dB (no margin and no channel coding)<sup>4,6</sup>. The subchannels with  $SNR$  smaller than 14.5 dB will not be used. As regulated by the DMT-ADSL standard,<sup>2</sup> the symbol error probability at either the real or the imaginary part should be less than  $10^{-7}$ , *i.e.*  $\frac{P_s}{2} < 10^{-7}$ . Assume that the real and the imaginary part of noise in a target subchannel is extremely high, and its normalized noise covariance matrix is equal to

$$\mathbf{C}_k = \begin{pmatrix} 1 & 0.95 \\ 0.95 & 1 \end{pmatrix}.$$

From (17), we can calculate the maximum noise distance  $d_{k,max} \approx 7.58$ . The minimum distance between the received symbols is  $\Delta_k \approx 7.51$ , which can be calculated according to (20).

This situation is depicted in Fig. 5, where the solid constellation point is the transmitted symbol. The transmitted symbol is located in the center of a circle with radius  $d_{k,max}$ . This circle covers only 4 constellation points, if the symbol error rate is less than  $2 \times 10^{-7}$ . Thus, we can perform symbol-by-symbol ML decision by considering only the four closest constellation points of the received symbol. The probability that the received symbol is not within the circle is smaller than  $2 \times 10^{-7}$ .

As  $\rho_k$  increases,  $d_{k,max}$  will increase as well. We are interested in knowing how large  $\rho_k$  can be so that  $d_{k,max}$  is large enough to cover both  $\mathbf{x}_k[m]$  and  $\mathbf{X}_k[n]$ . If the two points should be covered, decision making based only on the four closest constellation points is not adequate. Instead, six closest constellation points are needed in this situation. This can be illustrated as in Fig. 13, where  $\mathbf{x}_k[m]$  and  $\mathbf{X}_k[n]$  are covered in the circle.

Let us consider the case  $\sigma_{Re\{q_k\}}^2 = \sigma_{Im\{q_k\}}^2$ . By solving the triangular problem, we find that the circle will cover both  $\mathbf{x}_k[m]$  and  $\mathbf{x}_k[n]$  if  $d_{k,max} > 8.89$ . This can be seen in Fig. 13, where  $d_{k,max} = 8.89$ . According to Eqn. (17),  $d_{k,max} = 8.8$  when  $\rho_k = 0.999995$ . That is, even in a highly correlated noisy environment, the decision can be made by considering only the four closest constellation points of the received symbol. Therefore, when  $SNR_k > 14.5$  dB and  $P_s = 2 \times 10^{-7}$ , it is adequate to calculate the maximum likelihood function of four constellation points and then decide the most possible one. This result greatly reduces the complexity of symbol-by-symbol ML detection so that it can be practically used.

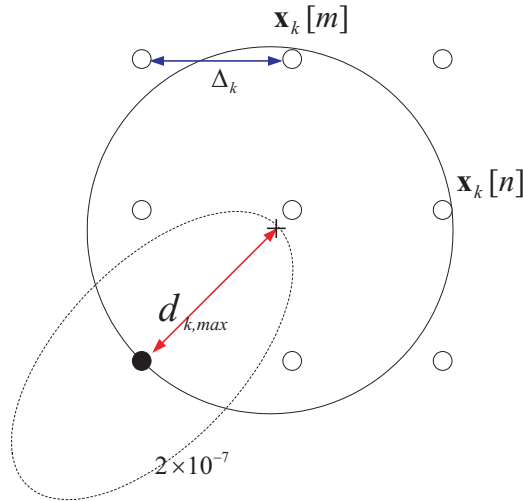


**Figure 13.** The relationship between  $d_{k,max}$  and  $\Delta_k$ .

## 5. CONCLUSION AND FUTURE WORK

A symbol-by-symbol maximum likelihood detection for DMT systems was proposed in this work. It was shown by simulation results that the scheme outperforms the symbol-by-symbol minimum distance detection by up to 2 dB. Furthermore, it was demonstrated that we only need to consider the four closest points of the received symbol at the cost of little performance degradation while the complexity can be greatly reduced. In the future, we will derive the bit allocation formula and consider Trellis-Coded Modulation (TCM) for the proposed scheme.

## REFERENCES

1. J. A. C. Bingham, "Multicarrier modulation for data transmission: an idea whose time has come," *IEEE Communications Magazine*, May 1990.
2. *Asymmetric Digital Subscriber Line Metallic Interface Standard T1.413*, American National Standards Institute, Aug. 1995.
3. J. S. Chow, J. C. Tu, J. M. Cioffi, "A discrete multitone transceiver system for HDSL applications," *IEEE Journal on Selected Areas in Communications*, vol. 9, Aug. 1991.
4. J. M. Cioffi, "A multicarrier prime," in *ANSI Doc., T1E1.4 Tech. Subcommittee, no. 91-157*, 1991.
5. J. S. Chow, *Finite-Length Equalization for Multi-Carrier Transmission Systems*, Ph. D. Dissertation of Stanford University, June 1992.
6. P. S. Chow and J. M. Cioffi, "Method and apparatus for adaptive, variable bandwidth, high-speed data transmission of a multicarrier signal over digital subscriber lines," *United States patent* No. 5479447, Dec. 1995.
7. Y. P. Lin and S. M. Phoong, "Perfect discrete multitone modulation with optimal transceivers," *IEEE Trans. Signal Processing*, vol. 48, Jun. 2000.
8. I. Djokovic, "MMSE equalizers for DMT systems with and without crosstalk," *IEEE conference record of the 31<sup>th</sup> Asilomar Conference on Signals, Systems & Computers*, Nov. 1997.